Medicine®

OPEN

Investigation on the mechanisms of guiqi huoxue capsule for treating cervical spondylosis based on network pharmacology and molecular docking

Yingying Liu, MM[a], Jingyuan Zhang, MM[a], Xinkui Liu, MM[a], Wei Zhou, MM[a], Antony Stalin, MM[b], Changgeng Fu, PhD[c], Jiarui Wu, PhD[a],*, Guoliang Cheng, MM[d], Siyu Guo, MM[a], Shanshan Jia, MM[a], Bingbing Li, PhD[c], Haojia Wang, MM[a], Jialin Li, MM[a], Shan Lu, MM[a]

Abstract

Background: Guiqi huoxue capsule (GQHXC) is a patented Chinese medicine used for treating a liver and kidney deficiency and blood stasis syndrome due to qi deficiency. It is caused by cervical spondylosis (cervical spondylotic radiculopathy (CSR), mixed cervical spondylosis mainly composed of nerve root type). Its underlying mechanisms need, however, to be further clarified.

Methods: In this study, collecting compounds, predicting therapeutic targets, constructing networks, and analyzing biological functions and pathways were based on network pharmacology analysis. In addition, molecular docking verification was engaged to assess the binding potential of selected target-compound pairs.

Results: We established 5 networks: compound-putative target network of GQHXC, protein-protein interaction (PPI) network related to CSR, compound-CSR target network, potential therapeutic targets PPI network, and herb-compound-target-pathway network. Network analysis indicated that 7 targets (tumor necrosis factor [TNF], interleukin 6 [IL6], nitric oxide synthase 3 [NOS3], Interleukin-8 [CXCL8], prostaglandin-endoperoxide synthase 2 [PTGS2], vascular endothelial growth factor A [VEGFA], and AP-1 transcription factor subunit [JUN]) might be the therapeutic targets of GQHXC in CSR. Moreover, molecular docking verification showed that TNF, IL6, NOS3, CXCL8, PTGS2, VEGFA, and JUN had a good is interaction with the corresponding compounds. Furthermore, enrichment analysis indicated that GQHXC might exert a curative role in CSR by regulating some important pathways, such as TNF signaling pathway, NF–kappa B signaling pathway, AGE–RAGE signaling pathway in diabetic complications, and so on.

Conclusion: Our study preliminarily explained the underlying mechanisms of GQHXC for treating CSR, and molecular docking verification was adopted as an additional verification. These findings laid a valuable foundation for experimental research and further application of GQHXC in the clinical treatment of CSR.

Abbreviations: BP = biological processes, CC = cell composition, CS = cervical spondylosis, CSR = cervical spondylotic radiculopathy, CXCL8 = Interleukin-8, GO = gene ontology, GQHXC = guiqi huoxue capsule, IL-1β = interleukin 1 beta, IL6 = interleukin 6, JUN = AP-1 transcription factor subunit, KEGG = kyoto encyclopedia of genes and genomes, MF = molecular function, NF-κB = transcription factor p65, NO = nitric oxide, NOS3 = nitric oxide synthase 3, PPI = protein-protein interaction, PTGS2 = prostaglandin-endoperoxide synthase 2, TCM = Traditional Chinese Medicine, TCMSP = Traditional Chinese Medicine Systems Pharmacology Database and Analysis Platform, TNF-α = tumor necrosis factor superfamily, member 2, TNF = tumor necrosis factor, VEGFA = vascular endothelial growth factor A.

---

1. Introduction

Cervical spondylosis (CS) is also called cervical vertebrae syndrome in medicine, which is a general term for cervical osteoarthritis, proliferative cervical spondylitis, cervical nerve root syndrome, and cervical disc herniation.[1] It is a degenerative joint disease, and the causes of the disease include degeneration, trauma, strain, inflammation, developmental spinal stenosis, and congenital deformity.[2] Generally, CS can be divided into different types such as neck type cervical spondylopathy, cervical spondylotic radiculopathy (CSR), cervical spondylotic myelopathy, vertebral artery type of cervical spondylosis, sympathetic type of cervical spondylosis, esophagus-type cervical spondylosis, and mixed cervical spondylosis.[3] CSR is one of the most common types of cervical spondylosis.[4,5] Traditional Chinese medicine (TCM) theory believes that the CS belongs to the category of "bi syndrome".[6] "BI syndrome" in traditional Chinese medicine refers to a disease characterized by pain, swelling, stiffness, deformation, and other symptoms and signs of limited movement in the body's joints and skeletal muscles.[7] Also, Vertigo, nuchal arthralgia, headache, and shoulder-neck pain tend to describe this disease.[8,9] The cause of CS is a clear orifice. The inducements are qi deficiency in clear orifice and meridians obstruction due to blood, which nature is asthenia in origin and asthenia in superficiality.[10,11] Treatment for CS include operative and non-operative methods. Non-operative methods include drug treatment, physical therapy, exercise therapy, small needle knife therapy, acupuncture therapy, and massage therapy.[12] Oral TCM therapy is an effective means of conservative treatment.[13,14]

Guiqi huoxue capsule (GQHXC) is a Chinese patent medicine composed of 13 Chinese herbal medicines: *Astragali Radix* (HQ), *Angelicae Sinensis Radix* (DG), *Paeoniae Radix Alba* (BS), *Polygoni Multiflori Radix Praeparata* (ZHSW), *Lycii Fructus* (GQZ), *Viscum Coloratum* (HJS), *Cervi Cornu Pantotrichum* (LR), *Drynariae Rhizoma* (GSB), *Clematidis Radix et Rhizoma* (WLX), *Tuberculate Speranskia Herb* (ZZTGC), Artificial Musk (RGSX), *Puerariae Lobatae Radix* (GG), *Chuanxiong Rhizoma* (CX). Its usage and dosage are as follows: orally, 3 capsules at a time, 3 times a day, and the course of treatment is 4 weeks.[16] The main effects of GQHXC are promoting blood circulation for removing obstruction in the channel, tonifying qi and tonifying the kidney.[15] According to TCM, qi is the most essential substance that constitutes the human body and the most essential substance that maintains the life activity of the human body.[16] GQHXC is used for treating a deficiency of both liver and kidney and blood stasis syndrome due to qi deficiency, which is caused by CS (CSR, mixed cervical spondylosis mainly composed of nerve root type).[15] This study focused on the network pharmacology of GQHXC for treating CSR. TCM obtains its superior therapeutic efficacy in the biological network of the human body system, which has the characteristics of multicomponent, multi-target, and multi-pathway synergism.[17] However, its medicinal basis and mechanism of action are unclear, making it difficult to carry out comprehensive system research from the general to the cellular and molecular level.[18] Based on

the "disease-gene-target-drug" interaction network, network pharmacology systematically and comprehensively observes the intervention and influence of drugs on the disease network, thus revealing the mystery of the synergetic effect of drugs in the human body.[17] The application of network pharmacology in the research of TCM conforms to the treatment, which is based on syndrome differentiation of the overall view of traditional Chinese medicine, and the characteristics of TCM include the multicomponent, multi-target, and multi-pathways.[19]

Chinese herbal medicines such as HQ, DG, CX, and RGSX have therapeutic effects on CSR.[20–22] Some literature suggests that GQHXC has therapeutic effects on CSR,[23–25] but its molecular mechanism has not fully been elucidated. Therefore, this study adopted network pharmacology to explore and predict the molecular mechanism of GQHXC against CSR. The detailed workflow of the network pharmacology research is illustrated in Figure 1.

2. Materials and methods

2.1. Collection of guiqi huoxue capsule active ingredients

To retrieve all the chemical components in GQHXC, we relied on TCM systems pharmacology Database and Analysis Platform (TCMSP, http://tcmspw.com/tcmsp.php), Shanghai Institute of Organic Chemistry of CAS (Chemistry Database [DB/OL], http://www.organchem.csdb.cn. [1978–2020]), China National Knowledge Infrastructure Database (CNKI, http://www.cnki.net/), and PubChem (https://pubchem.ncbi.nlm.nih.gov/). The relevant compounds were collected by entering the name of the Chinese herbal medicine into the TCMSP and Chemistry Database. Among them, LR, the compounds of ZHSW and ZZTGC were not found in the above database. Thus, research articles on components related to those Chinese herbal medicines were searched in CNKI to collect relevant compound information. A total of 980 compounds were collected, of which 87 were HQ, 125 were DG, 85 were BS, 24 were ZHSW,[26–34] 188 were GQZ, 40 were HJS, 72 were LR,[35,36] 71 were GSB, 57 were WLX, 11 were ZZTGC,[37–42] 13 were RGSX, 18 were GG, and 189 were CX. Finally, the collected compounds were integrated to screen the candidate compounds.

2.2. Candidate active compounds and related targets

After deleting duplicate data and compounds without structural information, 112 compounds were summarized (see Table S1, Supplemental Content, http://links.lww.com/MD2/A441 which illustrates the information of 112 active compounds) with oral bioavailability (OB) ≥30% and drug-likeness (DL) ≥0.18, which were regarded as candidate compounds. The numbers of active compounds in HQ, DG, BS, ZHSW, GQZ, HJS, LR, GSB, WLX, ZZTGC, RGSX, GG, and CX were 20, 2, 13, 4, 45, 7, 6, 18, 7, 3, 2, 4, and 7, respectively. Table S1, http://links.lww.com/MD2/A441 lists the basic information of these compounds. After removing the
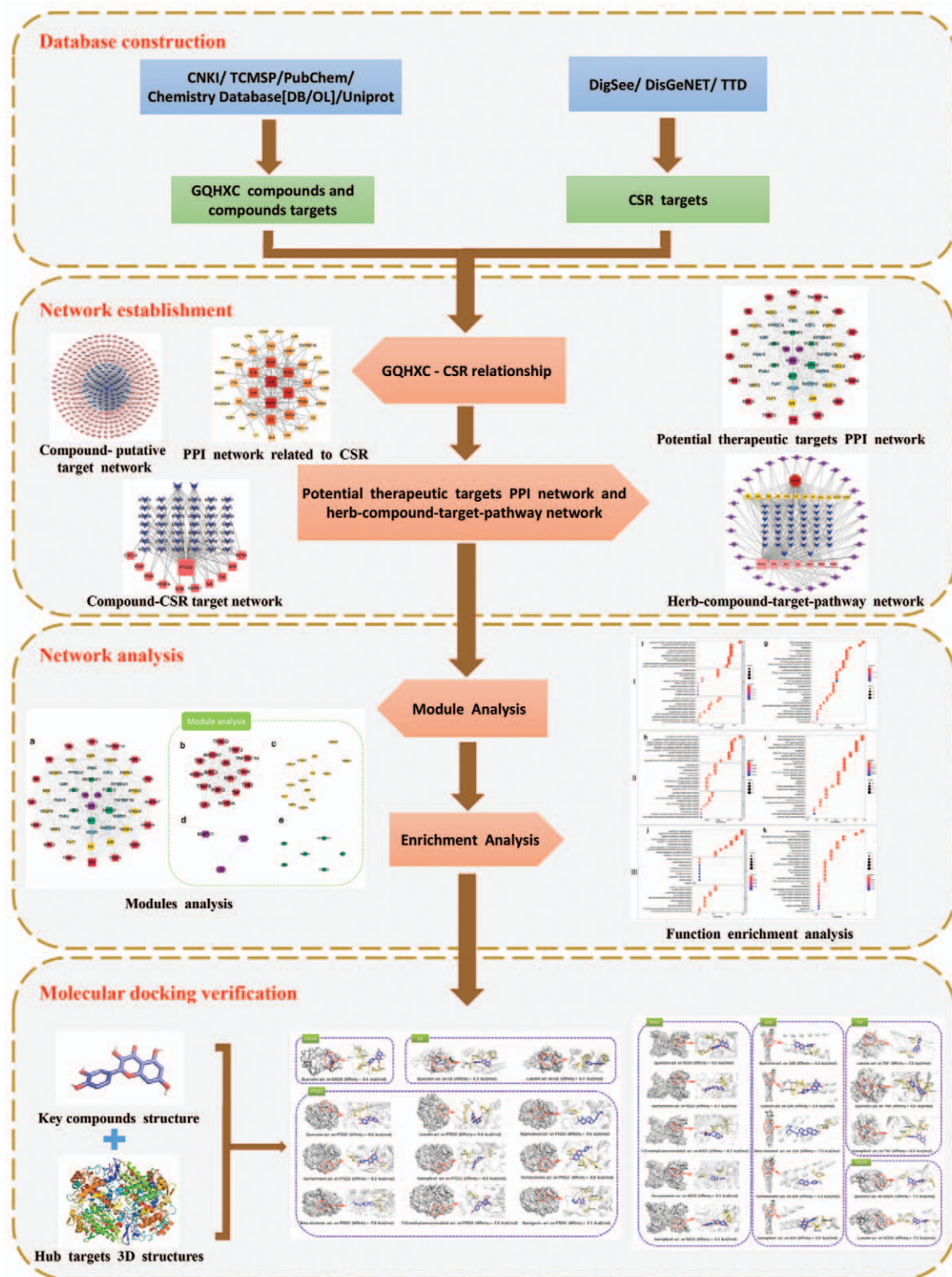
Figure 1. Workflow for GQHXC in the treatment of CSR.

compounds with no corresponding targets, 84 compounds were retained. There are 260 targets associated with them. In addition, the targets of these compounds were obtained through TCMSP. The Uniprot database (https://www.uniprot.org/) was utilized to find corresponding genes.

2.3. Cervical spondylotic radiculopathy targets

The target search terms used were "Cervical spondylotic radiculopathy," "cervical spondylosis of nerve root type," "nerve root cervical spondylosis" and "nerve root cervical spondylopathy" to find the targets in the disease gene search

engine (http://210.107.182.61/geneSearch/),[43] DisGeNET (http://www.disgenet.org/search),[44] and Therapeutic Target Database (, https://db.idrblab.org/ttd/).[45] Finally, we obtained 57 protein targets of CSR.

2.4. Construction of protein-protein interaction network

PPI data were collected from the STRING database (Search Tool for the Retrieval of Interacting Genes/Proteins, https://string-db.org/), which is known for predicted interactions, including direct and indirect interactions of proteins.[46] The confidence ranges of PPIs are defined by the database for interaction score (low confidence: score <0.4; medium confidence: 0.4–0.7; high confidence: > 0.7). When related targets were entered into the search tool for the retrieval of interacting genes database, we selected the high confidence, and the species was limited to "Homo sapiens". Furthermore, "the 1st shell" and "the 2nd shell" were set to "no more than 20 interactors" in potential therapeutic targets PPI network.

2.5. Network establishment

All the above networks were constructed based on Cytoscape 3.7.2 software (http://www.cytoscape.org/), an open-source software platform, which is made available for interactive network analysis, integration, and visualization of networks and network data.[47] In the interaction network, each node has a meaningful parameter "Degree" to evaluate its topological characteristics.[48] There is a positive correlation between the degree value and the importance of the node in the networks. The following 5 networks were established in this study.

1. Compound-putative target network of GQHXC: This network was built by contacting candidate active compounds of GQHXC and corresponding targets.
2. PPI network related to CSR: The PPI network was established by linking CSR-related targets and other human proteins that connected or interacted with CSR targets.
3. Compound-CSR target network: The above 2 networks were intersected to build this network by the merge function in Cytoscape 3.7.2.
4. Potential therapeutic targets PPI network: This PPI network was constructed by linking the proteins obtained from the network of (3) and other related humans proteins.
5. Herb-compound-target-pathway network: The comprehensive network was based on connecting herbs, compounds, corresponding targets, and pathways.

There is a positive proportional relationship between the node size and degree of networks.

2.6. Gene ontology functional enrichment analysis and kyoto encyclopedia of genes and genomes pathway enrichment analysis

To evaluate the role of the key potential targets in gene function and signaling pathway, gene ontology (GO) knowledgebase (http://geneontology.org/),[49] kyoto encyclopedia of genes and genomes (KEGG) pathway enrichment analysis (https://www.genome.jp/kegg/) were performed using the R 3.6.1 software (https://cran.r-project.org/doc/FAQ/R-FAQ.html#Citing-R) with the Bioconductor package.[50] Both the P value and q-value parameters are set to less than .01.

2.7. Molecular docking verification

AutoDockTools 1.5.6 was employed to perform the docking analysis. The compounds were retrieved from TCMSP and Pubchem database and the target proteins retrieved from the protein data bank database (https://www.rcsb.org/),[51] For the ligand and proteins, the parameters such as rotatable bonds, merging charge, dehydration, and hydrogenation were set by default. The screening conditions were set as follows:

1. the protein structure is obtained by X-crystal diffraction;
2. the crystal resolution of the protein is less than 3 Å;
3. preferential selection of protein structures reported in the literature related to molecular docking;
4. the organism comes from Homo sapiens.

Based on the above conditions, 7 core target protein protein data bank IDs were gathered, and the water molecules and co-crystallized pro-ligand molecules were removed by the Notepad++ (https://notepad-plus-plus.org/) and AutoDockTools.

Subsequently, the format of a compound and target protein was converted into *pdbqt format in Auto Dock software. Finally, molecular docking calculations were performed using Autodock Vina 1.1.2.[52] The PyMol 2.3.2 (https://pymol.org/2/) software was wielded to visualize the docking results.[53,54] The negative binding energy (<0) indicates that the ligand and the receptor can spontaneously bind without consuming energy. At present, there is no uniform standard for the target screening of active molecules. According to the literature report,[55] the active ingredients has been selected with a binding energy of −5.0 kcal/mol or less as the basis for screening GQHXC therapeutic targets. To better analyze the docking results, we took the binding energy and the active pocket of the target predicted by POCASA 1.1 (http://altair.sci.hokudai.ac.jp/g6/service/pocasa/) into consideration.

3. Results

3.1. Compound-putative target network of guiqi huoxue capsule

As shown in Figure 2, the compound-putative target network of GQHXC includes 344 nodes (84 compounds and 260 targets) and 928 edges (see Table S2, Supplemental Content, http://links.lww.com/MD2/A442 which illustrates the information of nodes in the compound-putative target network of GQHXC). In addition, each edge represents an interaction between compound molecules and targets. The degree of a node is equal to the number of edges connected to the node in the network, and the size of the node is positively related to the degree value. The average degree value of the nodes in this network was 5.4, the average number of targets per compound was 12, and each target interacted with an average of 4 compounds. Thus, in GQHXC, we not only found that 1 compound can interact with multiple targets but also different compounds can work together on the same target. These findings reflected the mechanism of interaction between multiple components and multiple targets of GQHXC. From a compound perspective, 28.57% of the compounds interact with 10 or more targets, and 18 compounds can interact with 20 or more targets. Among them, quercetin in HQ and GQZ has the highest degree of connectivity and can interact with 145 target proteins. It is followed by kaempferol, luteolin, and 7-O-methylisomucronulatol, which can interact with 58 targets, 57 targets, and 41 targets, respectively. Besides, isorhamnetin, formononetin, beta-sitosterol, and naringenin can interact with
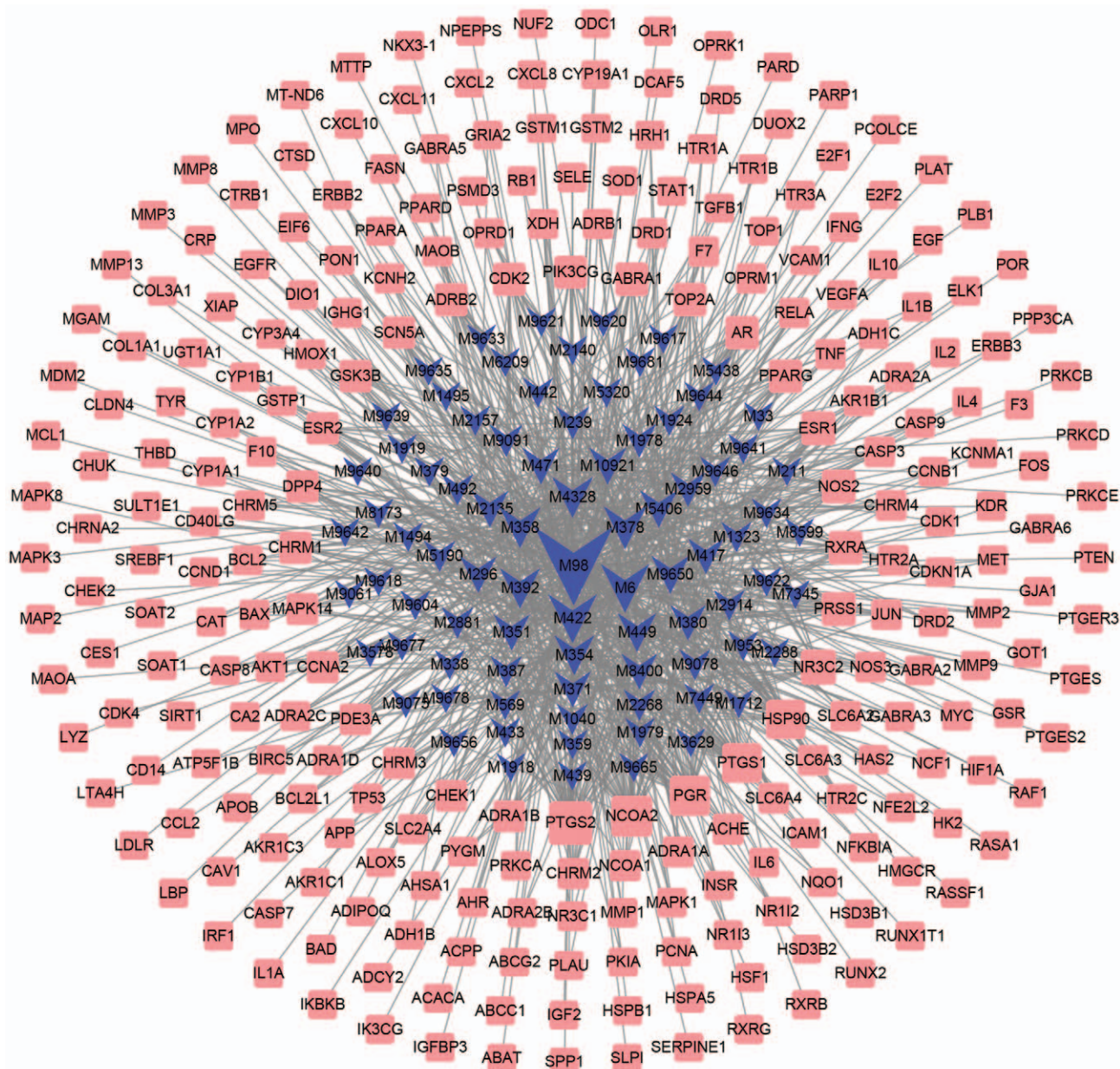
Figure 2. Compound-putative target network of GQHXC. Blue nodes represent compounds in GQHXC. Pink nodes represent corresponding targets [drawn by Cytoscape 3.7.2 (https://cytoscape.org/)].

more than 30 target proteins. For the targets, 5 targets can interact with 20 or more compounds. The highest degree value was PTGS2 corresponding to 43 compounds, followed by NCOA2, which corresponded to 36 compounds; PGR corresponded to 34 compounds, PTGS1 corresponded to 32, and HSP90 corresponded to 31. These corresponding interactions also explain the pharmacological mechanism of the multiple components and multiple targets of GQHXC.

3.2. Protein-protein interaction network related to cervical spondylotic radiculopathy

The 57 CSR-related target proteins were entered into the String 11.0 database for search, and protein interaction relationship data with a high-confidence interval score >0.7 was selected to ensure

the reliability of the data. Then, the retrieved data was imported into Cytoscape 3.7.2 software to build a PPI network (Fig. 3). PPI network related to CSR included 40 CSR-related proteins and 125 interactions among CSR-related proteins (see Table S3, Supplemental Content, http://links.lww.com/MD2/A443 which illustrates the topology characteristics of nodes from the PPI network related to CSR). There are 15 nodes with a degree value greater than the average degree value of 6.25 in the network.

3.3. Compound- cervical spondylotic radiculopathy target network

After linking the compound-putative target network of GQHXC with the PPI network related to CSR using the merge function in Cytoscape 3.7.2, 11 potential targets (vascular endothelial
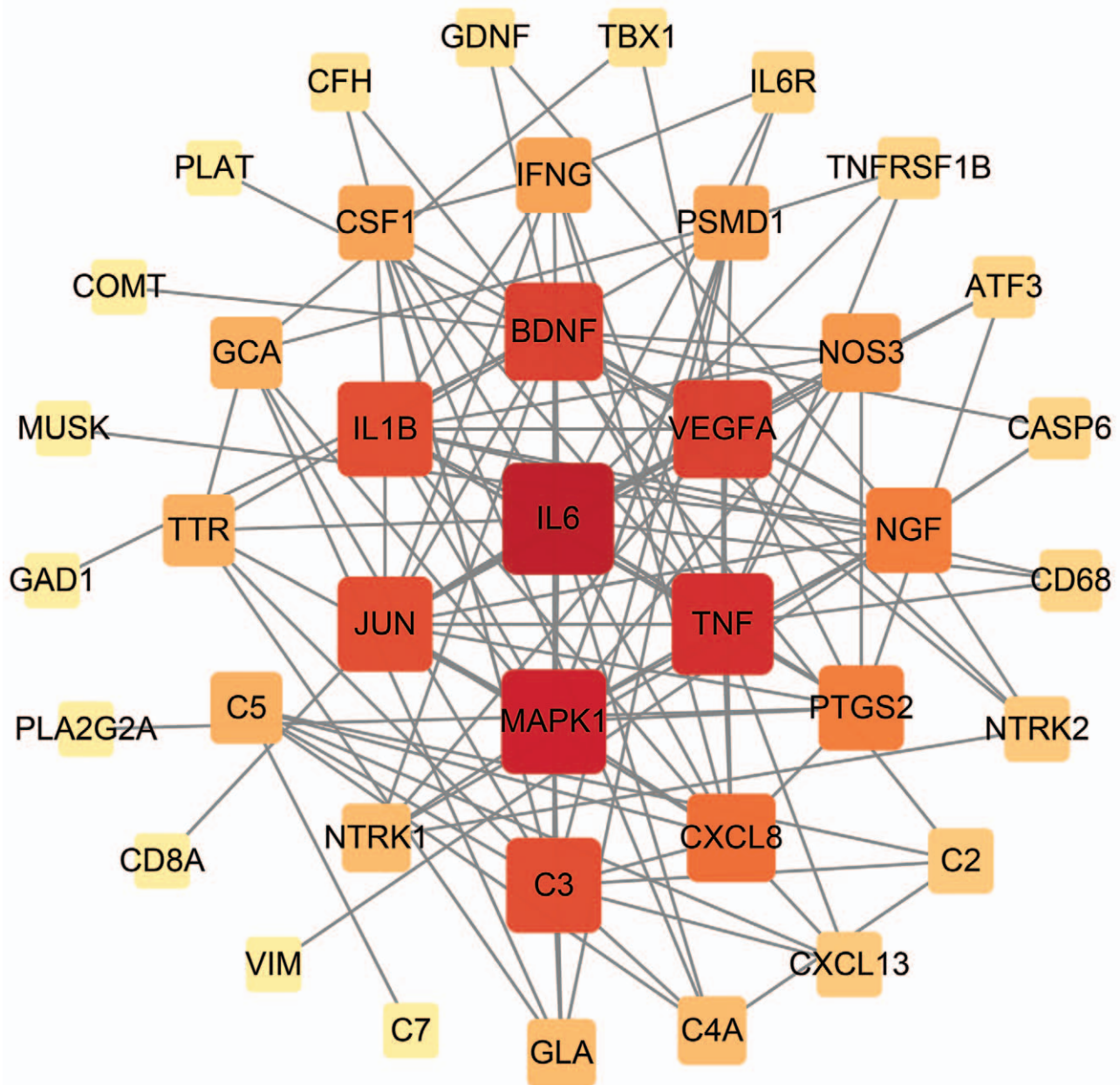
Figure 3. PPI network related to CSR. There is a positive proportional relationship between the degree and color [drawn by Cytoscape 3.7.2 (https://cytoscape.org/)].

growth factor A [VEGFA], mitogen-activated protein kinase 1, AP-1 transcription factor subunit [JUN], tumor necrosis factor [TNF], IL6, Tissue-type plasminogen activator, prostaglandin-endoperoxide synthase 2 [PTGS2], interferon gamma, IL1B, CXCL8, nitric oxide synthase 3 [NOS3]) for GQHXC treatment of CSR were intuitively obtained. The connection principle among nodes is that when the predicted targets of the active ingredients in GQHXC were the same as the targets of the CSR, the predicted targets were associated with the targets of the CSR, and these linked targets were considered as potential targets for the treatment of CSR by GQHXC. The compound-CSR target network was shown in Figure 4 (see Table S4, Supplemental Content, http://links.lww.com/MD2/A444 which illustrates the topology characteristics of nodes from the Compound-CSR

target network). There are 6 proteins (PTGS2, NOS3, JUN, TNF, IL6, mitogen-activated protein kinase 1) with a degree value greater than or equal to an average degree value of 2.69, and the highest degree value of PTGS2 is 43, which means that they are likely to be considered as the key therapeutic targets for GQHXC for treating CSR. The degree value of quercetin, luteolin, kaempferol, aloe-emodin, and formononetin was 11, 7, 4, 3, and 3, respectively, which are all higher than the average degree. They are expected to be the main active ingredients for treating CSR.

3.4. Module analysis of potential therapeutic targets protein-protein interaction network

The 11 potential targets obtained in the Compound-CSR target network (3.3) were entered into the String 11.0 database with
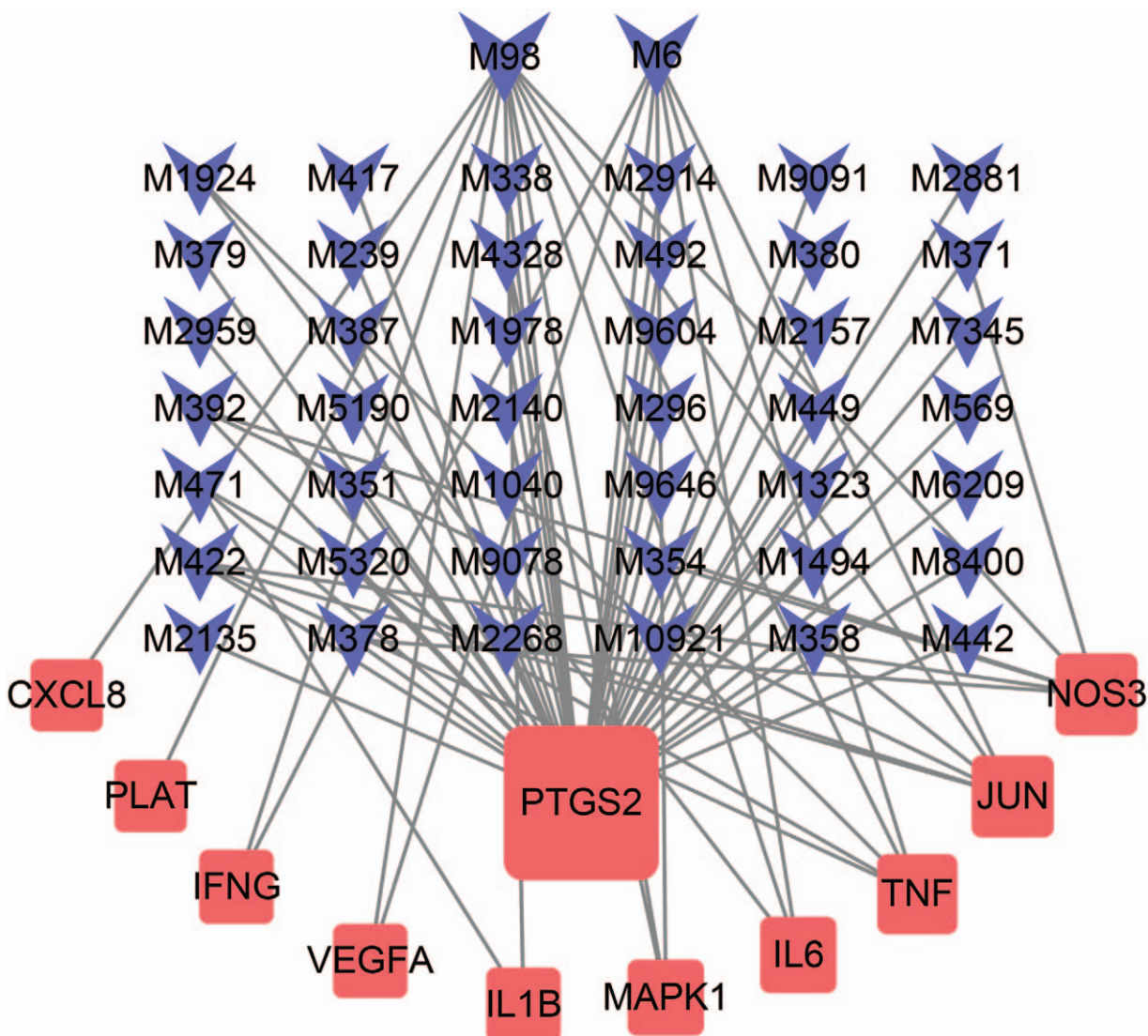
Figure 4. Compound-CSR target network. Blue nodes represent compounds in GQHXC. Pink nodes represent potential targets for GQHXC in the treatment of CSR [drawn by Cytoscape 3.7.2 (https://cytoscape.org/)].

high confidence of parameter, and the "1st shell" and "the 2nd shell" were set to "no more than 20 interactors". The species was limited to "Homo sapiens" and high confidence was selected. The collected data were then imported into Cytoscape 3.7.2, and the molecular complex detection function was utilized to perform a module analysis on potential targets. Potential therapeutic targets PPI network is shown in Figure 5A (see Table S5, Supplemental Content, http://links.lww.com/MD2/A445 which illustrates the information of nodes in the Potential therapeutic targets PPI network). Four modules were obtained through clustering the network. Module 1 (Fig. 5B) has 16 nodes and 115 edges, and module 2 has 14 nodes and 43 edges. The degree value of 68.75% of target proteins in module 1 was greater than the average degree value of 14.375. The degree value of 35.71% of target proteins in module 2 (Fig. 5C) was higher than the average degree value of 6.14. 7 targets (TNF, VEGFA, JUN, NOS3, IL6, CXCL8, and PTGS2) were identified from module 1 and module 2 as the predicted most critical targets. Module 3 (Fig. 5D) has 3 nodes and 3 edges, and module 4 (Fig. 5E) has 6 nodes and 7 edges. We

selected module 1 and module 2 with higher scores for the subsequent analysis.

3.5. Gene ontology function enrichment and kyoto encyclopedia of genes and genomes pathway enrichment analysis

We used R 3.6.1 (https://cran.r-project.org/doc/FAQ/R-FAQ. html#Citing-R) software to perform GO and KEGG enrichment analysis on the protein targets of the 3 networks in (a) (b) and (c) in Figure 5 (see Table S6, Supplemental Content, http://links.lww. com/MD2/A446 which illustrates the list of GO enrichment results to genes in all enrichment analysis; see Table S7, Supplemental Content, http://links.lww.com/MD2/A447 which illustrates the list of pathway enrichment results to genes in all enrichment analysis). In the bubble chart, the X-axis represents the number of target genes (Gene Ratio), and the Y-axis represents the KEGG pathway or GO term where the target gene is significantly enriched. The size of the dots intuitively reflects the
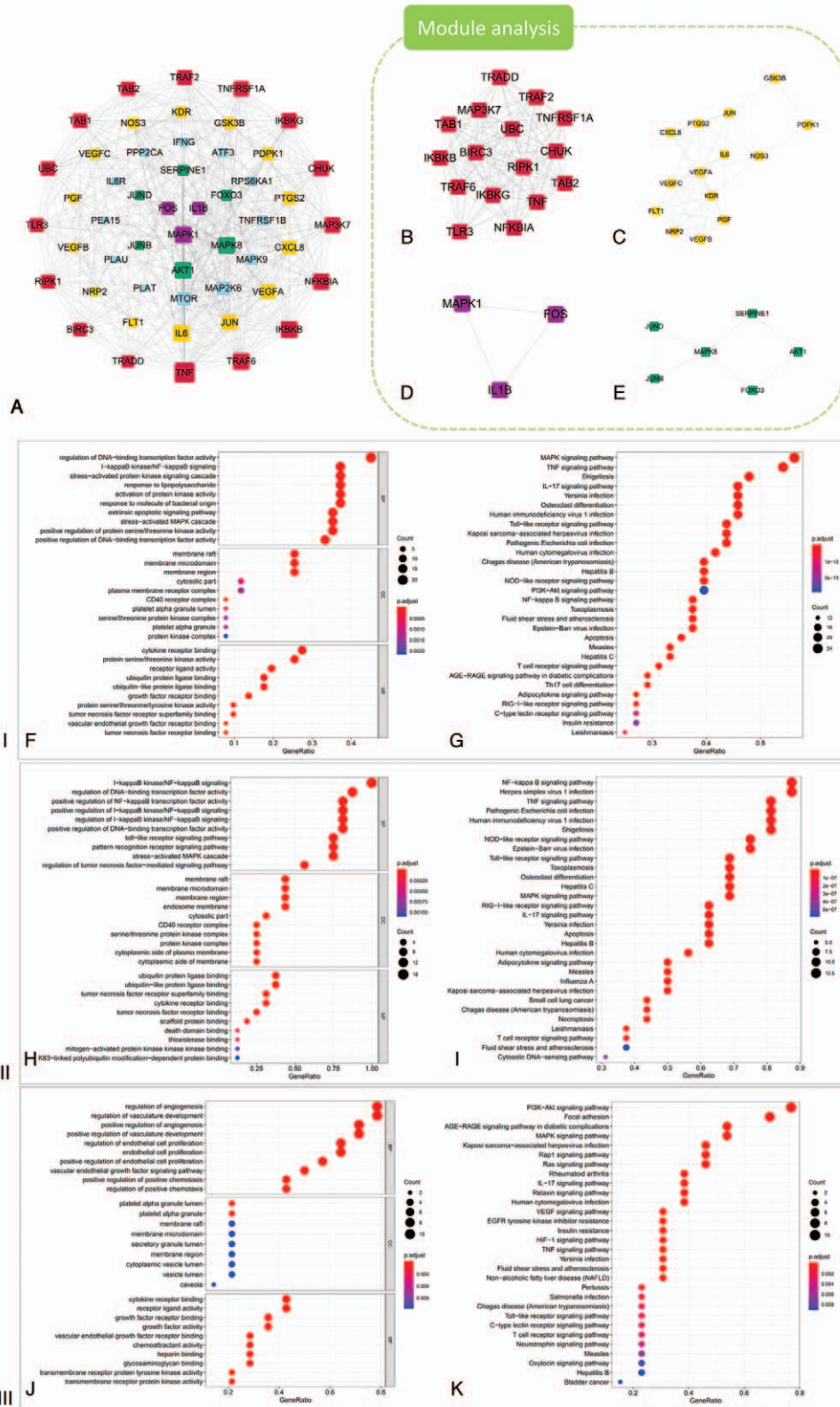
Figure 5. (A): Potential therapeutic targets PPI network. Red nodes represent module 1, yellow nodes represent module 2, purple nodes represent module 3, and green nodes represent module 4 [drawn by Cytoscape 3.7.2 (https://cytoscape.org/)]. The size of the nodes is directly proportional to the degree of the nodes. (B): Module 1 (Score = 15.333). (C): Module 2 (Score = 6.615). (D): Module 3 (Score = 3). (E): Module 4 (Score = 2.8). (F): GO enrichment analysis for potential therapeutic targets PPI network. (G): KEGG pathway analysis for potential therapeutic targets PPI network. (H): GO enrichment analysis for module 1. (I): KEGG pathway analysis for module 1. (J): GO enrichment analysis for module 2. (K): KEGG pathway analysis for module 2. Top 30 KEGG pathways were shown in the figure, *P* value <.01 and q-value<0.01. Top 10 GO terms were shown in the figure, *P* value <.01 and q-value<0.01. Functional enrichment analysis is drawn by R 3.6.1(https://cran.r-project.org/doc/FAQ/R-FAQ.html#Citing-R).

size of the Gene Ratio, and the color depth of the dots reflects different p-value ranges.

1. Analysis of potential therapeutic targets PPI network: In the GO enrichment analysis (Fig. 5F), a total of 954 terms were found, of which 913 terms were related to biological processes (BP), 15 terms were related to cell composition (CC), and 26 terms were related to molecular function (MF). KEGG pathway enrichment analysis (Fig. 5G) found 180 pathways, of which 113 pathways had a *P* value and q-value less than .01.

2. Analysis of module 1: In the GO enrichment analysis (Fig. 5H), a total of 303 terms were found, of which 277 terms were related to BP, 12 terms were related to CC, and 14 terms were related to MF. KEGG pathway enrichment analysis (Fig. 5I) found 97 pathways, of which 56 pathways had a *P* value and q-value less than .01.

3. Analysis of module 2: In the GO enrichment analysis (Fig. 5J), a total of 125 terms were found, of which 192 terms were related to BP, 9 terms were related to CC, and 14 terms were related to MF. KEGG pathway enrichment analysis (Fig. 5K) found 130 pathways, of which 41 pathways had a *P* value and q-value less than .01.

3.6. Herb-compound-target-pathway network

Herb-compound-target-pathway network (Fig. 6A) consists of 94 nodes and 277 edges (7 nodes of key potential targets, 30 nodes of the pathway, 44 nodes of the compound, 12 nodes of herbs, and 1 of "GQHXC"). For the pathways, the degree value of the AGE-RAGE signaling pathway in diabetic complications was 6, and the degree value of Human cytomegalovirus infection, Kaposi sarcoma-associated herpesvirus infection, and IL-17 signaling pathway was 5. From the analysis of the target protein, PTGS2 degree value was 50, TNF degree value was 31, JUN degree value was 28, and IL6 degree value was 20. The highest degree value of quercetin in the compound was 8, the degree

value of luteolin was 6, the degree value of kaempferol was 5, and finally the degree value of formononetin was 4.

The pathological processes of CSR are closely associated with inflammatory responses and blood vessels. Seven putative targets and transcription factor p65 [NF-κB] are the most active factors that participate in these key pathways, which imply an important role in the occurrence and promotion of CSR. KEGG Database (https://www.kegg.jp/kegg/kegg1.html) and software of Pathway Builder Tool 2.0 were used to generate the figure. As showed in Figure 6B, putative major signaling pathways of GQHXC were constructed.

3.7. Molecular docking verification

We initially selected 44 compounds and the 7 target proteins in Figure 6A as ligands and receptors for molecular docking verification. We then selected the top 10 of the 44 compounds ranked according to the degree value in table S2, http://links.lww.com/MD2/A442 as the final ligands. Because Atropine belongs to table S2, http://links.lww.com/MD2/A442 but did not belong to these 44 compounds, the final docking ligands were 9 (quercetin, luteolin, kaempferol, beta-sitosterol, formononetin, isorhamnetin, 7-O-methylisomucronulatol, Stigmasterol, and naringenin). The active pockets of target proteins were predicted on the POCASA 1.1 website. VEGFA and JUN target proteins did not receive any active prediction sites on the website, so their docking results were selected for the successful docking and highest score. For the target proteins in the activity prediction pocket, the docking results with the highest score and success in the active site were selected. The lower the affinity between compound and target, the better the binding activity between them. As shown in Table 1, 27 pairs of target-compound combinations were delivered to Vina for docking, and their docking score was less than or equal to -5.3 kcal/mol, which indicates that they have good binding activity. We can conclude that PTGS2 and NOS3 have a better affinity with the corresponding compound. Using Pymol software, these compounds were observed to enter the
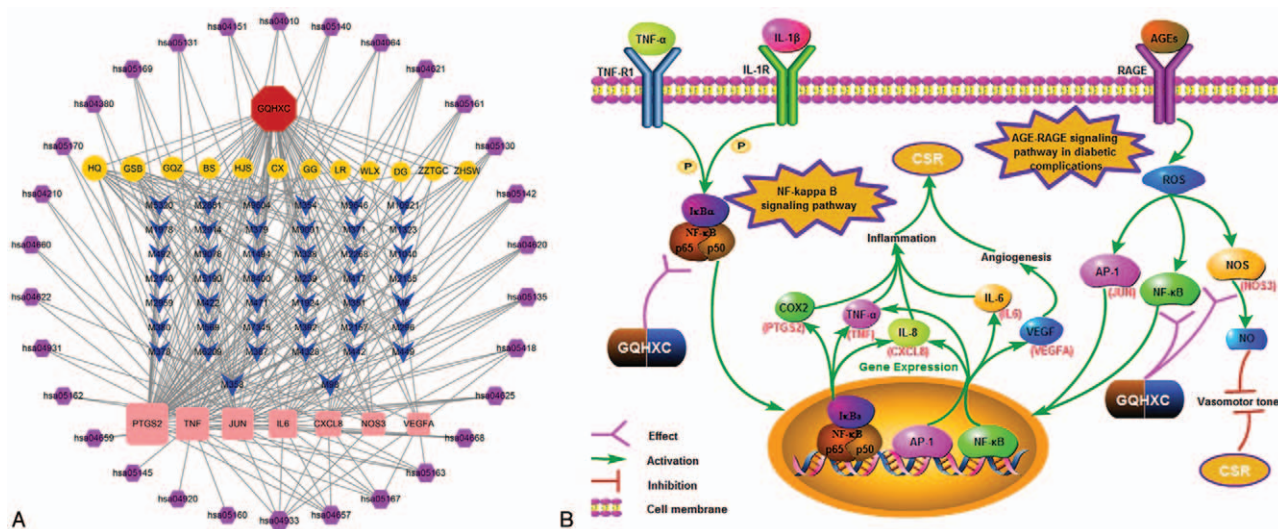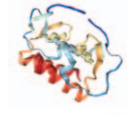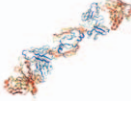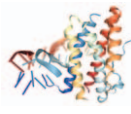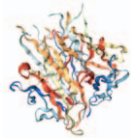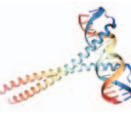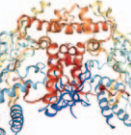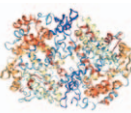
Figure 6. (A): Herb-compound-target-pathway network. Red node represents "GQHXC". Yellow nodes represent herbs. Pink nodes represent potential targets of GQHXC in the treatment of CSR. Blue nodes represent compounds. Purple nodes represent pathways [drawn by Cytoscape 3.7.2 (https://cytoscape.org/)]. (B): Illustration of crucial putative biological progress caused by putative targets for CSR. Red labels are targets related to products of gene expression.

Table 1

Information of molecular docking.

Proteins	PDB ID	Protein structure	Test compounds	TCMSPMID	Affinity (kcal/mol)
CXCL8	6N2U		Quercetin	MOL000098	−5.6
VEGFA	6BFT		Quercetin	MOL000098	−7.4
			Luteolin	MOL000006	−7.9
IL6	4NI7		Quercetin	MOL000098	−6.3
			Luteolin	MOL000006	−6.4
TNF	6OOY		Quercetin	MOL000098	−6.6
JUN	5T01		Luteolin	MOL000006	−7.0
			Kaempferol	MOL000422	−6.4
			Quercetin	MOL000098	−5.3
			Luteolin	MOL000006	−5.9
			Kaempferol	MOL000422	−5.8
			beta-Sitosterol	MOL000358	−7.0
			Formononetin	MOL000392	−5.9
NOS3	6CIE		Quercetin	MOL000098	−9.0
			Kaempferol	MOL000422	−9.6
			formononetin	MOL000392	−9.5
			Isorhamnetin	MOL000354	−9.7
			7-O-methylisomucronulatol	MOL000378	−8.2
PTGS2	5IKV		Quercetin	MOL000098	−9.6
			Luteolin	MOL000006	-9.6
			Kaempferol	MOL000422	−8.9
			beta-Sitosterol	MOL000358	−7.8
			Formononetin	MOL000392	−8.8
			Isorhamnetin	MOL000354	−9.2
			7-O-methylisomucronulatol	MOL000378	−7.2
			Stigmasterol	MOL000449	−9.6
			Naringenin	MOL004328	−7.1

active pocket of the protein. Detailed verification target-compound interactions were given in Figure 7.

4. Discussion

Owing to the complexity of GQHXC components, its mechanism for treating CSR has not yet been elucidated. In this study, a network pharmacological approach was used to determine the pharmacological mechanism of potential compounds and targets in GQHXC on CSR. Therefore, the compound-putative target network of GQHXC, PPI network related to CSR, compound-CSR target network, potential therapeutic targets PPI network, and the herb-compound-target-pathway network, were established to systematically analyze the mechanism of GQHXC action on CSR. It is well known that after CSR occurs, a large

number of inflammatory factors are released at the damaged tissue, which mediate nerve root pain.[56] Some studies have shown that the pathogenesis of CSR is closely related to the expression of pro-inflammatory factors such as IL-1, IL-6, IL-18, interleukin 1 beta [IL-1β], and TNF-α,[57–61]. It is also related to the content of nitric oxide (NO), ET (endothelin), IgA, IgM, IgG, C3, C4, PGE2(prostaglandin E2), and so on in plasma.[62–65] CSR is increased by the release of PGE2, a pro-inflammatory mediator.[62] The disease progression of CSR will be exacerbated when the activity of NO decreases and excessive secretion of ET.[63] C3 and C4 in CSR patients are lower than in normal people, while IgA, IgM, and IgG are higher than in normal people.[64]

The network pharmacology study predicted the following 7 potential targets: TNF, VEGFA, JUN, NOS3, IL6, CXCL8, and
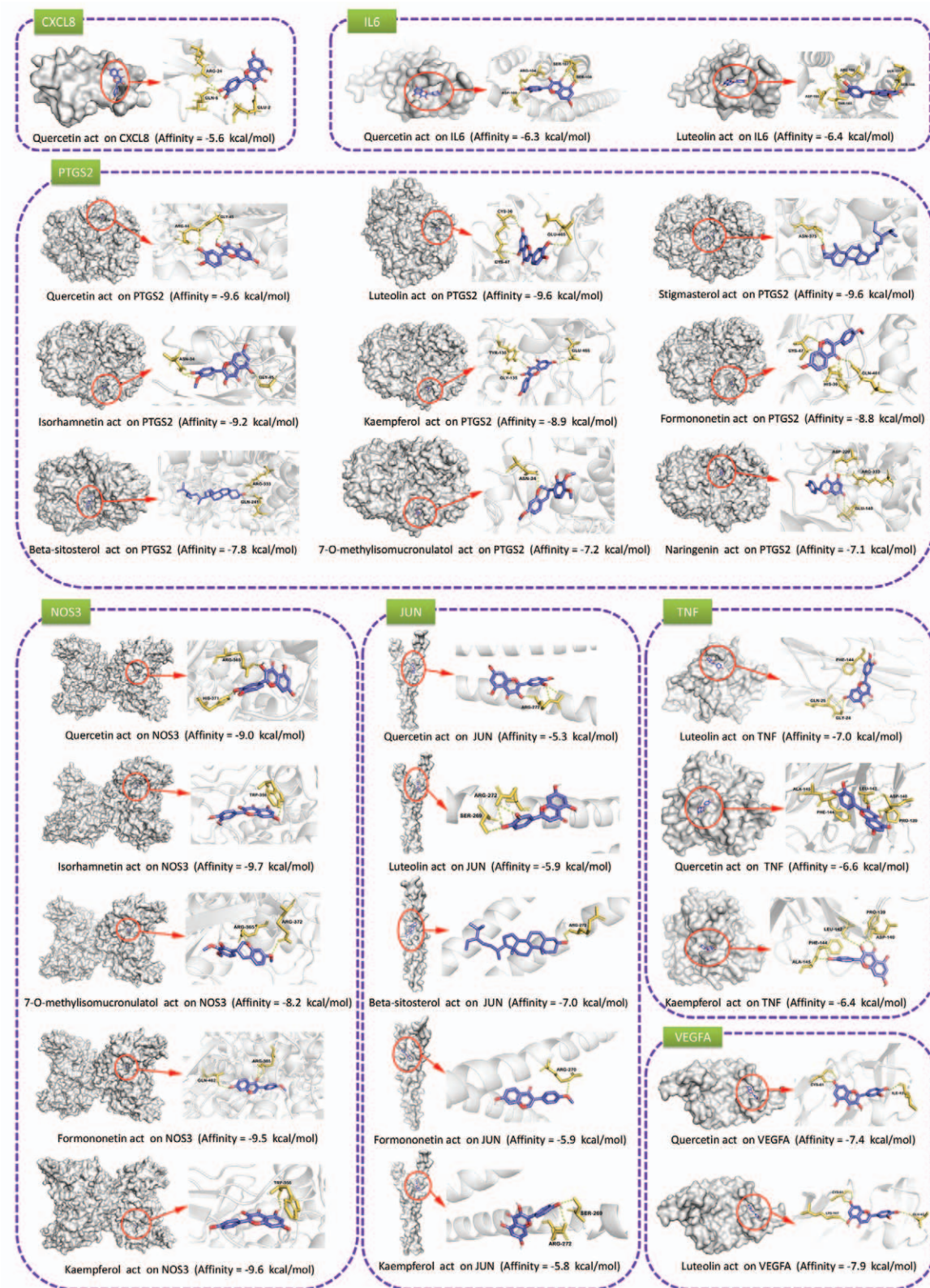
Figure 7. Detailed target-compound interactions of the molecular docking verification. Green rectangles represent the targets and the pictures in the round square are the docking verification of each target.

PTGS2, which may be the key targets for GQHXC for treating CSR. PTGS2 is responsible for the prostanoid biosynthesis involved in inflammation and mitogenesis. PTGS2 may additionally be associated with activating the NF kappa B signaling pathway.[66] PTGS2 is an essential target for nonsteroidal anti-inflammatory drugs, and down-regulating PTGS2 expression can help reduce the inflammatory response.[67] PTGS2 is a key enzyme for PGE2 formation, which affects the release of PGE2. The protein encoded by CXCL8 is a significant mediator of the inflammatory response. The encoded protein is secreted primarily by neutrophils, where it serves as a chemotactic factor by guiding the neutrophils to the site of infection.[68] This chemokine is also a potent angiogenic factor.[69] VEGFA is a member of the PDGF/VEGF growth factor family. It encodes a heparin-binding protein, which exists as a disulfide-linked homodimer.[70] This growth factor induces proliferation and migration of vascular endothelial cells and has an essential role in physiological and pathological angiogenesis.[71] Furthermore, VEGFA expression may be regulated by PI3K/AKT pathway.[72] The TNF gene encodes a multifunctional proinflammatory cytokine that belongs to the TNF superfamily. This cytokine participates in regulating a broad spectrum of biological processes, including cell proliferation, differentiation, apoptosis, lipid metabolism, and coagulation.[73] TNF gene transcription produces inflammatory factors such as TNF-α. Its production is generally the combination of some stimulating factors such as LPS and specific receptors of monocytes or macrophages.[74] These stimulating factors activate transcription factors through a series of signal transduction and initiate downstream TNF gene transcription.[75] IL6 gene encodes a cytokine that functions in inflammation and the maturation of B cells.[76] The protein is primarily produced at sites of acute and chronic inflammation, where it is secreted into the serum and induces a transcriptional inflammatory response through the interleukin 6 receptor, alpha.[77] The functioning of this gene is implicated in a wide variety of inflammation-associated disease states IL-6.[78] JUN is linked to human malignant tumors.[79] Variations in the NOS3 are made in association with susceptibility to coronary spasm.[80] NO mediates vasodilation, and the release of NO is regulated by endothelial NOS3.[81] CSR pathogenesis is associated with inflammation and blood vessels, and these possible key targets can regulate inflammatory factors and angiogenesis. From the above analysis, it can be recognized that the 7 targets screened in this study have relevant research support.

By analyzing the compound-putative target network of GQHXC and the herb-compound-target-pathway network, 9 target compounds (quercetin, luteolin, kaempferol, beta-sitosterol, formononetin, 7-O-methylisomucronulatol, stigmasterol, isorhamnetin, naringenin) are considered as the key components of GQHXC for treating CSR. For example, quercetin can block the activation of NF-κB, a transcription factor associated with the inflammatory response, and inhibit the production of inflammatory factors. At the same time, it also inhibits the generation of blood vessels.[82] S. H. Kim observed that kaempferol not only can suppress the release of NO and PGE2 but also reduce the expression levels of tumor necrosis factor superfamily, member 2 (TNF-α) and NF-κB.[83] Luteolin and quercetin have obvious inhibitory effects on IL-6 and TNF-α and have beneficial anti-inflammatory effects.[84,85] F. Yao verified that beta-sitosterol could reduce the content of TNF-α and IL-6 in BALF of ALI mice and down-regulate the activation of NF-κB p65 signal transduction pathway.[86] Furthermore, formononetin can significantly

reduce the expression of inducible nitric oxide synthase, TNF-α and IL-1β, and other inflammatory factors.[87] Another study suggested that kaempferol, quercetin, and isorhamnetin inhibit iNOS protein and mRNA expression and NO production in a dose-dependent manner, thereby inhibiting the activation of NF-κB.[88] This is a significant transcription factor of iNOS, which plays a role in anti-inflammatory and protecting the integrity of vascular endothelium. Stigmasterol can inhibit the degradation of various inflammatory mediators and matrices and exert its inhibitory effect by blocking the IL-1β-induced NF-κB pathway.[89] MAPK signaling pathway in MCF-7 cells can be inhibited by naringenin,[90] while PI3K/Akt signaling protein can be activated.[91] Even though there are no large literature reports on 7-O-methylisomucronulatol, it has good oral bioavailability (OB=74.69%) and drug-like properties (DL=0.30). It can be perceived that the 9 screened key compounds mainly affect inflammatory response. Theoretically, they can reduce the inflammatory factors released at the tissues damaged by CSR, ameliorate inflammation and pain, and regulate angiogenesis and vascular tone.

In this study, we performed GO enrichment analysis to elucidate various mechanisms of GQHXC treatment of CSR at a systemic level. The bubble chart showed that the BP enrichment results of modules 1 and 2 are better than CC and MF. From thatwe can know that GQHXC mainly treats CSR through biological processes. BP entries in module 1 include regulations of I-kappaB kinase / NF-kappaB signaling, DNA–binding transcription factor activity, and tumor necrosis factor–mediated signaling pathway. In addition, the positive regulations of NF–kappaB transcription factor activity, DNA–binding transcription factor activity, and I–kappaB kinase/NF–kappaB signaling are also included in GO entries.

Furthermore they also included stress–activated MAPK cascade, pattern recognition receptor, and toll–like receptor signaling pathways. The I–kappaB kinase/NF–kappaB signaling not only ranks first in the GO entries but also some of the above-mentioned related regulations are related to it. These BP entries are mainly involved in the regulation of the inflammatory response. It is believed that GQHXC can treat the damaged tissues of CSR patients. BP entries in module 2 include positive regulations of angiogenesis, positive chemotaxis, endothelial cell proliferation, and vasculature development. Additionally here were the regulations of vasculature development, positive chemotaxis, angiogenesis regulation of positive chemotaxis, and endothelial cell proliferation. Vascular endothelial growth factor signaling pathways and endothelial cell proliferation were also among the GO entries. BP entries in module 2 are mainly involved in the regulations of angiogenesis and vascular endothelium. We speculated that this is related to the regulation of NO, ET, IgA, IgM, IgG, PGE2, etc. in the plasma of CSR patients.

From KEGG enrichment analysis of module 1, we found that most of the pathways involved inflammation and immunity, such as the NF-kappa B signaling pathway, NOD-like receptor signaling pathway, RIG-I-like receptor signaling pathway, and so on. In addition, it is speculated that Shigellosis, Pathogenic Escherichia coli, Herpes simplex virus 1, and other infections are related to inflammation. There are vascular-related pathways in module 2, such as the VEGF signaling pathway, Oxytocin signaling pathway, and Relaxin signaling pathway. The Ras signaling pathway, Rap1 signaling pathway, focal adhesion, and EGFR tyrosine kinase inhibitor resistance are linked with cell

regulation. Pathways in both modules such as MAPK signaling pathway, Toll-like receptor signaling pathway, IL-17 signaling pathway, T cell receptor signaling pathway, and TNF signaling pathway, are all connected with inflammation and immunity. The infections in both modules are also detected in association with inflammation. Thus we can see that the results of the KEGG enrichment analysis of inflammation and immunity in these 2 modules are very useful. There are pathways related to blood vessels and cell regulation in module 2. For instance, the AGE-RAGE signaling pathway can activate NF-κB and stimulate the production of vascular endothelial growth factor VEGF.[92] Focal plaques are constituted by the interconnection of extracellular membrane adhesion molecules (ECM), integrin on the cell membrane, and intracellular cytoskeleton proteins. Adhesive plaques have functions of mechanical structure and signal transmission, which can maintain the normal structure of cells and exert their normal functions.[93] Quercetin can exert anti-inflammatory and immune regulation effects by inhibiting MAPK and NF-κB signaling pathways.[94] Formononetin can regulate the PI3K-Akt pathway, VEGF pathway, and MAPK signaling pathway to intervene in the inflammatory response.[95] We speculate that the components of GQHXC may play an important role in treating CSR through key factors of these signaling pathways.

Although our research discussed the molecular mechanism of GQHXC, there are still some limitations. First, research data comes from existing databases, so the authenticity and completeness of the results depend on the quality of the data. Second, the results do not reflect all the natural cellular network characteristics in the organism, so further experiments will be needed to confirm the presented data.

5. Conclusion

In this study, 9 active compounds and 7 key genes were selected using network pharmacology. The enrichment analysis of GO and KEGG was conducted to find the potential mechanism of GQHXC in the treatment of CSR. In conclusion, we predicted that GQHXC affects the inflammatory response and vascular regulation process and may achieve the goal of curing CSR. Further experiments are, however, needed to confirm the results of this prediction in GQHXC.

Author contributions

Conceptualization: Jiarui Wu.
Data curation: Changgeng Fu, Siyu Guo.
Formal analysis: Shanshan Jia, Bingbing Li, Haojia Wang, Jialin Li, Shan Lu.
Methodology: Xinkui Liu, Wei Zhou, Guoliang Cheng.
Supervision: Jiarui Wu, Guoliang Cheng.
Writing – original draft: Yingying Liu.
Writing – review & editing: Yingying Liu, Jingyuan Zhang, Antony Stalin.

References

[1] Jia SL. Research progress and prospect of cervical spondylosis. Orthoped J Chin 2001;1:5–6.
[2] Zhao GS, Zhang Q, Quan ZX. Mid-term efficacy and safety of cervical disc arthroplasty versus fusion in cervical spondylosis: a systematic review and meta-analysis. Biomed Rep 2017;6:159–66.
[3] Yu J, Zhu LG. Research status of recurrent cervical spondylotic radiculopathy. Beijing J Tradit Chin Med 2013;32:892–6.
[4] Radhakrishnan K, Litchy WJ, O'Fallon WM, Kurland LT. Epidemiology of cervical radiculopathy. A population-based study from Rochester, Minnesota, 1976 through 1990. Brain 1994;117(Pt 2):325–35.
[5] Kim HJ, Nemani VM, Piyaskulkaew C, Vargas SR, Riew KD. Cervical radiculopathy: incidence and treatment of 1,420 consecutive cases. Asian Spine J 2016;10:231–7.
[6] Dong FH. Precise application of Traditional Chinese Medicine in minimally-invasive techniques. Zhongguo Gu Shang 2018;31:493–6.
[7] Zhang SH, Yang YF, Shi Y. Study on theoretical framework of etiology and pathogenesis of bi syndrome. J Liaoning Univers Tradit Chin Med 2020;22:54–6.
[8] Cui XJ, Sun YL, You SF, et al. Effects of Qishe Pill, a compound traditional Chinese herbal medicine, on cervical radiculopathy: study protocol for a randomized controlled trial. Trials 2013;14:322.
[9] Yang L, Yang C, Pang X, et al. Mechanoreceptors in diseased cervical intervertebral disc and vertigo. Spine (Phila Pa 1976) 2017;42:540–6.
[10] Yang F, Tan MS, Yi P, Tang XS, Hao QY, Qi YN. Clinical study on spinal cord decompression combined with traditional Chinese medicine for the treatment of cervical spondylotic myelopathy. Zhongguo Gu Shang 2018;31:30–6.
[11] Zhang J, Yi JG, Sun SC. Overview of traditional Chinese medicine in the treatment of cervical spondylotic radiculopathy. J Tradit Chin Med (Beijing, China) 1997;38:435–7.
[12] Zuo G, Gao TC, Xue BH, et al. Assessment of the efficacy of acupuncture and chiropractic on treating cervical spondylosis radiculopathy: a systematic review and meta-analysis. Medicine (Baltimore) 2019;98: e17974.
[13] Cui X, Trinh K, Wang YJ. Chinese herbal medicine for chronic neck pain due to cervical degenerative disc disease. Cochrane Database Syst Rev 2010;2010:CD006556.
[14] Carette S, Fehlings MG. Clinical practice. Cervical radiculopathy. N Engl J Med 2005;353:392–9.
[15] China Medical Information Platform. Available at: https://www.dayi.org.cn/drug/1022657 [Accessed April 2, 2020].
[16] Tian TL. Discussion on "Qi stagnation as pathological product". Jiangsu J Traditi Chin Med 2007;1:69.
[17] Li S, Zhang B. Traditional Chinese medicine network pharmacology: theory, methodology and application. Chin J Nat Med 2013;11:110–20.
[18] Luo TT, Lu Y, Yan SK, Xiao X, Rong XL, Guo J. Network pharmacology in research of Chinese medicine formula: methodology, application and prospective. Chin J Integr Med 2020;26:72–80.
[19] Muhammad J, Khan A, Ali A, et al. Network pharmacology: exploring the resources and methodologies. Curr Top Med Chem 2018;18:949–64.
[20] Zhang Y, Wang C, Guo Y. Of clinical reseach on cervical spondylosis treated with acupoint injection in recent five years. Zhongguo Zhen Jiu 2012;32:477–9.
[21] Zhou J, Liu F, Jiang W, Hu M. Cost-effectiveness of Jingshu granules compared to placebo for the treatment of patients with cervical radiculopathy in China: a decision-tree model based on randomized controlled trial. J Altern Complement Med 2019;25:1183–92.
[22] Boyd A, Bleakley C, Hurley DA, et al. Herbal medicinal products or preparations for neuropathic pain. Cochrane Database Syst Rev 2019;4: CD010528.
[23] Xu CG. Observation on clinical therapeutic effect of Guiqi Huoxue capsule combined with glucosamine sulfate in the treatment of cervical spondylosis. World Chin Med 2019;14:2313–5. 2319.
[24] Zhou Y. Clinical experimental study of flunarizine combined with Guiqi Huoxue capsule in the treatment of cervical spondylosis. Nei Mongol J Traditi Chin Med 2014;33:65–6.

[25] Cheng GL, Jiang YL, Li BB, Luo L. Effects of guiqi huoxue capsule in cervical spondylosis model rats. World Chin Med 2020;15:2369–72.

[26] Yu J, Xie J, Mao XJ, et al. Hepatoxicity of major constituents and extractions of radix polygoni multiflori and radix polygoni multiflori praeparata. J Ethnopharmacol 2011;137:1291–9.

[27] Yan Y, Hao Y, Hu S, Chen X, Bai X. Hollow fibre cell fishing with high performance liquid chromatography for screening bioactive anthraquinones from traditional Chinese medicines. J Chromatogr A 2013;1322:8–17.

[28] Yu J, Xie J, Mao XJ, et al. Comparison of laxative and antioxidant activities of raw, processed and fermented Polygoni Multiflori radix. Chin J Nat Med 2012;10:63–7.

[29] Zhang J, Xu W, Wang P, et al. Chemical analysis and multi-component determination in Chinese medicine preparation Bupi Yishen formula using ultra-high performance liquid chromatography with linear ion trap-orbitrap mass spectrometry and triple-quadrupole tandem mass spectrometry. Front Pharmacol 2018;9:568.

[30] Ma J, Zheng L, He YS, Li HJ. Hepatotoxic assessment of Polygoni Multiflori Radix extract and toxicokinetic study of stilbene glucoside and anthraquinones in rats. J Ethnopharmacol 2015;162:61–8.

[31] Xing Y, Wang L, Wang C, et al. Pharmacokinetic studies unveiled the drug-drug interaction between trans-2,3,5,4'-tetrahydroxystilbene-2-O-β-d-glucopyranoside and emodin that may contribute to the idiosyncratic hepatotoxicity of Polygoni Multiflori Radix. J Pharm Biomed Anal 2019;164:672–80.

[32] Zhang Z, Yang L, Huang X, Gao Y. Metabolomics profiling of Polygoni Multiflori Radix and Polygoni Multiflori Radix Preparata extracts using UPLC-Q/TOF-MS. Chin Med 2019;14:175–7.

[33] Yang N, Cao FJ, Huo JW, et al. SREBP1-based active component screening of anthraquinones Radix Polygoni Multiflori Preparata for lowering lipid metabolism in hepatocellular carcinoma cells. J Hubei Univers Med 2018;37:156–60.

[34] Yu Y, Li JX, Jin Y, Ma FL, Yang J, Guo LP. Determination of 9 stilbene glycosides in Polygonum multiflorum by UPLC-MS /MS. J Chin Med Materials 2018;41:1395–8.

[35] Wang YH, Sun YS, Zhang L, Liu C, Gong RZ. Research on chemical compositions in different processed products of cervi cornu pantotrichum. Zhongguo Zhong Yao Za Zhi 2018;43:1145–55.

[36] Lv JW, Li JF, Bian XF, Zhang NX, Zhang H, Sun JM. Study on pilose antler network pharmacology based on "Ingredients-Targets-Pathways". Modern Chin Med 2019;21:1236–41.

[37] Lv R, Wei FF, He WW, Jin L. Content determination of total flavones in Herb Speranskiae Tuberculatae in different producing areas in Gansu Province. J Traditi Chin Veterinary Med 2019;38:46–9.

[38] Shen G, Jing DS, Yang F, Chen J, Ge R, Yang GE. Correlation analysis between HPLC fingerprint and anti-inflammatory activity of Speranskiae tuberculatae herba. Chine J Exp Traditi Med Formulae 2019;25:174–80.

[39] Gao HX, Lu RH, Wei XN, Wang HQ, Kong J. Analysis of the volatile oil from Tougucao. Chin Traditi Herbal Drugs 2000;1:16–7.

[40] Wang D, Sun JM, Wang GJ, Zhang H. Measuring total flavonoids in speranskia tuberculata using UV. Modernization of Traditional Chinese Medicine and Materia Medica-World Science and Technology 2007;1:61–3.

[41] Li C, Zhang CZ, Hu FD, Shi JG. Chemical constituents from Speranskia tuberculata (Bge) Baill. Zhongguo Zhong Yao Za Zhi 2000;25:291–2.

[42] Wang X, Zhang Y, Cai S, et al. Identification of Tougucao derived from Clematis species. Zhongguo Zhong Yao Za Zhi 1998;23:198–254.

[43] Kim J, So S, Lee HJ, Park JC, Kim JJ, Lee H. DigSee: disease gene search engine with evidence sentences (version cancer). Nucleic Acids Res 2013;41:W510–7.

[44] Piñero J, Bravo À, Queralt-Rosinach N, et al. DisGeNET: a comprehensive platform integrating information on human disease-associated genes and variants. Nucleic Acids Res 2017;45(D1):D833–9.

[45] Yang H, Qin C, Li YH, et al. Therapeutic target database update 2016: enriched resource for bench to clinical drug target and targeted pathway information. Nucleic Acids Res 2016;44(D1):D1069–74.

[46] Szklarczyk D, Morris JH, Cook H, et al. The STRING database in 2017: quality-controlled protein-protein association networks, made broadly accessible. Nucleic Acids Res 2017;45(D1):D362–8.

[47] Demchak B, Otasek D, Pico AR, et al. The cytoscape automation app article collection. F1000Res 2018;7:800.

[48] Meng Z, Liu X, Wu J, et al. Mechanisms of compound kushen injection for the treatment of lung cancer based on network pharmacology. Evid Based Complement Alternat Med 2019;2019:4637839.

[49] Wu Y, Li X, Liu J, Luo XJ, Yao YG. SZDB2.0: an updated comprehensive resource for schizophrenia research. Hum Genet 2020;139:1285–97.

[50] Kanehisa M, Goto S. KEGG: kyoto encyclopedia of genes and genomes. Nucleic Acids Res 2000;28:27–30.

[51] Goodsell DS, Zardecki C, Di Costanzo L, et al. RCSB protein data bank: enabling biomedical research and drug discovery. Protein Sci 2020;29:52–65.

[52] Trott O, Olson AJ. AutoDock Vina: improving the speed and accuracy of docking with a new scoring function, efficient optimization, and multithreading. J Comput Chem 2010;31:455–61.

[53] Yuan S, Chan HCS, Filipek S, Vogel H. PyMOL and inkscape bridge the data and the data visualization. Structure 2016;24:2041–2.

[54] Viegas DJ, Edwards TG, Bloom DC, Abreu PA. Virtual screening identified compounds that bind to cyclin dependent kinase 2 and prevent herpes simplex virus type 1 replication and reactivation in neurons. Antiviral Res 2019;172:104621.

[55] Liu X, Shi D, Zhou S, Liu H, Liu H, Yao X. Molecular dynamics simulations and novel drug discovery. Expert Opin Drug Discov 2018;13:23–37.

[56] Andrade P, Hoogland G, Garcia MA, Steinbusch HW, Daemen MA, Visser-Vandewalle V. Elevated IL-1β and IL-6 levels in lumbar herniated discs in patients with sciatic pain. Eur Spine J 2013;22:714–20.

[57] Pan SL, Zheng SL, Zhou XH, Wang QL. Acupuncture combined with Jingtong granule for nerve-root type cervical spondylosis and its effects on IL-6, TNF-α, IL-1β and hemorheological indexes. Zhongguo Zhen Jiu 2019;39:1274–8.

[58] Sun W, Zheng K, Liu B, et al. Neuroprotective potential of gentongping in rat model of cervical spondylotic radiculopathy targeting PPAR-γ pathway. J Immunol Res 2017;2017:9152960.

[59] Nascimento de Souza R, Silva FK, Alves de Medeiros M. Bee venom acupuncture reduces interleukin-6, increases interleukin-10, and induces locomotor recovery in a model of spinal cord compression. J Acupunct Meridian Stud 2017;10:204–10.

[60] Ozaktay AC, Kallakuri S, Takebayashi T, et al. Effects of interleukin-1 beta, interleukin-6, and tumor necrosis factor on sensitivity of dorsal root ganglion and peripheral receptive fields in rats. Eur Spine J 2006;15:1529–37.

[61] Solovieva S, Lohiniva J, Leino-Arjas P, et al. Intervertebral disc degeneration in relation to the COL9A3 and the IL-1ss gene polymorphisms. Eur Spine J 2006;15:613–9.

[62] Ulmann L, Hirbec H, Rassendren F. P2X4 receptors mediate PGE2 release by tissue-resident macrophages and initiate inflammatory pain. EMBO J 2010;29:2290–300.

[63] He XL. Effects of using Guben Shujin decoction combined with traction and acupoint iontophoresis in the treatment of nerve root type cervical spondylosis and the influence on electrophysiological indexes and plasma NO and ET Levels. J Sichuan Traditi Chin Med 2018;36:127–30.

[64] Xu SR, Jiang ZB, Zhang AM, Zhou ZH, He RL, Ye XL. Effect and mechanism of gabapentin in treating cervical spondylotic radiculopathy. Shandong Med J 2016;56:42–4.

[65] Liu GW, Wang XY, Meng XW, et al. Clinical observations on the efficacy of acupuncture at four tian points in treating cervical spondylosis of nerve root type. Shanghai J Acupunct Moxibustion 2009;28:25–8.

[66] Zhang X, Qu P, Zhao H, Zhao T, Cao N. COX-2 promotes epithelial-mesenchymal transition and migration in osteosarcoma MG-63 cells via PI3K/AKT/NF-κB signaling. Mol Med Rep 2019;20:3811–9.

[67] Ulrich CM, Whitton J, Yu JH, et al. PTGS2 (COX-2) -765G > C promoter variant reduces risk of colorectal adenoma among nonusers of nonsteroidal anti-inflammatory drugs [published correction appears in Cancer Epidemiol Biomarkers Prev. 2005 Dec;14(12):3020]. Cancer Epidemiol Biomarkers Prev 2005;14:616–9.

[68] Schutyser E, Struyf S, Proost P, et al. Identification of biologically active chemokine isoforms from ascitic fluid and elevated levels of CCL18/pulmonary and activation-regulated chemokine in ovarian carcinoma. J Biol Chem 2002;277:24584–93.

[69] Naito Y, Yamamoto Y, Sakamoto N, et al. Cancer extracellular vesicles contribute to stromal heterogeneity by inducing chemokines in cancer-associated fibroblasts. Oncogene 2019;38:5566–79.

[70] Dixelius J, Olsson AK, Thulin A, Lee C, Johansson I, Claesson-Welsh L. Minimal active domain and mechanism of action of the angiogenesis inhibitor histidine-rich glycoprotein. Cancer Res 2006;66:2089–97.

[71] Murphy JF, Fitzgerald DJ. Vascular endothelial growth factor induces cyclooxygenase-dependent proliferation of endothelial cells via the VEGF-2 receptor. FASEB J 2001;15:1667–9.

[72] Li L, Liu F, Huang W, et al. Ricolinostat (ACY-1215) inhibits VEGF expression via PI3K/AKT pathway and promotes apoptosis in osteoarthritic osteoblasts. Biomed Pharmacother 2019;118:109357.

[73] Liu T, Luo X, Li ZH, Wu JC, Luo SZ, Xu MY. Zinc-α2-glycoprotein 1 attenuates non-alcoholic fatty liver disease by negatively regulating tumour necrosis factor-α. World J Gastroenterol 2019;25:5451–68.

[74] Naime ACA, Bonfitto PHL, Solon C, et al. Tumor necrosis factor alpha has a crucial role in increased reactive oxygen species production in platelets of mice injected with lipopolysaccharide. Platelets 2019; 30:1047–52.

[75] Wang T, He C. TNF-α and IL-6: the link between immune and bone system. Curr Drug Targets 2020;21:213–27.

[76] Choy EH, De Benedetti F, Takeuchi T, Hashizume M, John MR, Kishimoto T. Translating IL-6 biology into effective treatments. Nat Rev Rheumatol 2020;16:335–45.

[77] Shibata C, Nakai K, Ozaki M, et al. Effects of interleukin-6 and tumor necrosis factor-α on the expression of angiogenic and collagenolytic factors in premature and mature adipocytes. Biochem Biophys Res Commun 2020;531:297–304.

[78] Lulińska-Kuklik E, Maculewicz E, Moska W, et al. Are IL1B, IL6 and IL6R gene variants associated with anterior cruciate ligament rupture susceptibility? J Sports Sci Med 2019;18:137–45.

[79] Chen Y, Zhu G, Liu Y, et al. O-GlcNAcylated c-Jun antagonizes ferroptosis via inhibiting GSH synthesis in liver cancer. Cell Signal 2019;63:109384.

[80] Gauer S, Balint B, Kollmann C, et al. Dysregulation of endothelial nitric oxide synthase does not depend on hemodynamic alterations in bicuspid aortic valve aortopathy. J Am Heart Assoc 2020;9:e016471.

[81] Bryan MT, Duckles H, Feng S, et al. Mechanoresponsive networks controlling vascular inflammation. Arterioscler Thromb Vasc Biol 2014; 34:2199–205.

[82] Ji JJ, Lin Y, Huang SS, Zhang HL, Diao YP, Li K. Quercetin: a potential natural drug for adjuvant treatment of rheumatoid arthritis. Afr J Tradit Complement Altern Med 2013;10:418–21.

[83] Kim SH, Park JG, Lee J, et al. The dietary flavonoid Kaempferol mediates anti-inflammatory responses via the Src, Syk, IRAK1, and IRAK4 molecular targets. Mediators Inflamm 2015;2015:904142.

[84] Lodhi S, Vadnere GP, Patil KD, Patil TP. Protective effects of luteolin on injury induced inflammation through reduction of tissue uric acid and pro-inflammatory cytokines in rats. J Tradit Complement Med 2019; 10:60–9.

[85] Laczko R, Chang A, Watanabe L, et al. Anti-inflammatory activities of Waltheria indica extracts by modulating expression of IL-1B, TNF-α, TNFRII and NF-κB in human macrophages. Inflammopharmacology 2020;28:525–40.

[86] Yao F, Zhou QY, Xiong Y, Guan S. Protective effects of β-Sitosterol on acute lung injury induced by lipopolysaccharide in mice. Chin Agricultural Sci Bulletin 2015;31:55–61.

[87] Gu MH, Hong W, Tang CQ, Li W, Gu Y. Formononetin protects blood-brain barrier and inhibits neuroinflammation during focal cerebral ischemia and reperfusion. J Jinan Univers 2015;36:34–9.

[88] Hämäläinen M, Nieminen R, Vuorela P, Heinonen M, Moilanen E. Anti-inflammatory effects of flavonoids: genistein, kaempferol, quercetin, and daidzein inhibit STAT-1 and NF-kappaB activations, whereas flavone, isorhamnetin, naringenin, and pelargonidin inhibit only NF-kappaB activation along with their inhibitory effect on iNOS expression and NO production in activated macrophages. Mediators Inflamm 2007; 2007:45673.

[89] Gabay O, Sanchez C, Salvat C, et al. Stigmasterol: a phytosterol with potential anti-osteoarthritic properties. Osteoarthritis Cartilage 2010; 18:106–16.

[90] Eanes L, Patel YM. Inhibition of the MAPK pathway alone is insufficient to account for all of the cytotoxic effects of naringenin in MCF-7 breast cancer cells. Biochim Open 2016;3:64–71.

[91] Zhang S, Jiang ZF, Pan Q, Song CY, Zhang WH. Anti-cancer effect of naringenin chalcone is mediated via the induction of autophagy, apoptosis and activation of PI3K/Akt signalling pathway. Bangladesh J Pharmacol 2016;11:684–90.

[92] Giurdanella G, Lazzara F, Caporarello N, et al. Sulodexide prevents activation of the PLA2/COX-2/VEGF inflammatory pathway in human retinal endothelial cells by blocking the effect of AGE/RAGE. Biochem Pharmacol 2017;142:145–54.

[93] Moll R, Bahn H, Bayerl C, Moll I. Zelluläre Adhäsionsmoleküle und Komponenten der extrazellulären Matrix als Zielstrukturen der Auto-immunität [Cellular adhesion molecules and components of the extracellular matrix as target structures of autoimmunity]. Pathologe 1996;17:254–61.

[94] Meng LQ, Yang FY, Wang MS, et al. Quercetin protects against chronic prostatitis in rat model through NF-κB and MAPK signaling pathways. Prostate 2018;78:790–800.

[95] Tay KC, Tan LT, Chan CK, et al. Formononetin: a review of its anticancer potentials and mechanisms. Front Pharmacol 2019;10:820.